

Hybrid Composites for the Design and Development of Pressure Vessel for Underwater Applications

A. Thirunavukkarasu^{#,*}, K. Shanmugasundaram[#] and G. Latha[§]

[#]Engineering Design Division, College of Engineering Guindy, Anna University, Chennai - 600 025, India

[§]Ocean Acoustics, National Institute of Ocean Technology, Ministry of Earth Sciences, Chennai - 600 100, India

*E-mail: vathiru.niot@gov.in

ABSTRACT

The study's main objective is to design and develop pressure vessels in underwater applications using Hybrid composites-Fibre Metal Laminates (FML) so that the weight will be reduced. The proposed pressure vessel accommodates electronics in the underwater ambient noise measurement system under an external hydrostatic pressure of 1 MPa (10 bar). The research study aims initially to design and develop a pressure vessel with stainless steel 316 L and subsequently design a pressure vessel with hybrid composites with a combination of composite materials of E-glass and carbon/epoxy materials with a metal alloy stainless steel 316 L. The pressure vessel has been optimised with varying metal and composite percentage combinations. The cylinder's wall thickness has been pivotal in optimizing pressure vessel design. Classical Laminate Theory (CLT) transforms the FML pressure vessel or cylinder into a rectangular plate. As preliminary measures, FML specimen with a size of 0.45 m square laminate and 0° orientation has been developed with 50 % metal layer and 50 % fibre composites, and corresponding mechanical tests have been carried out as per the standards. The tensile strength of the developed FML is 420 MPa compared to base metal (SS316 L) strength of 556 MPa, and similarly, Flexural and Impact properties have shown a higher level when compared to other types of FMLs.

Keywords: Fiber metal laminates; E-glass/epoxy; Carbon/epoxy; Classical laminate theory; External hydrostatic pressure

1. INTRODUCTION

Normally, the pressure vessel is cylindrical pressure housing used in underwater measurement systems like submersibles, marine echo-location systems and ambient noise measurements. In this study, the design and optimisation of pressure vessels for the underwater ambient noise measurement system have been considered and enumerated. In India, under the Ocean Acoustics program of the National Institute of Ocean Technology (NIOT), a subsurface system has been developed for the measurement of ambient noise in the ocean (Fig.1). The system has been operational in the Indian Seas for a decade including in the Arctic Region for the past five years¹. The purpose of the system is to record background noise in the ocean, and it consists of a data acquisition system with pressure vessel or pressure housing, hydrophone array and mooring components like acoustic release, anchor weight and buoyancy floats. The system is connected with a mooring mechanism and deployed below the sea surface. The pressure vessel with a rating of 1 MPa (10 bar) is necessary to house the electronics like data acquisition system, memory module and power pack for operations upto 100 m ocean depth. The performance of the pressure housing subjected to external pressure depends mainly on the proper selection of shape, size and material. A pressure vessel with a cylindrical shape is

mainly chosen for the axial load application. Considering the corrosive environment and the hydrostatic pressure prevailing in the ocean, primarily materials like Stainless Steel 316 L (SS316L), Aluminium 6061 and Titanium Gr-5 are considered to develop pressure vessels for underwater applications.

Fiber Metal Laminates (FML) are hybrid materials that combine Fiber Reinforced Plastics (FRP) and metallic materials. FMLs are hybrid composite materials with thin layers of metallic sheets and fibre-reinforced adhesives. In FMLs, the advantages of the excellent performance properties of FRP, such as high specific strength, high stiffness, good fatigue and anti-corrosion, are amalgamated with metal characteristics such as ductility, impact and damage resistance. Even though the FML are new group materials, their applications are limited due to technical complications involved in FRP adhesion and the materials high pricing. The significant applications of FMLs are in aerospace industries, automobile sectors, and construction engineering and marine structures. Initially, FML, namely ARALL (Aramid-Reinforced ALuminium Laminate) laminates, was introduced in 1978 in aerospace engineering at Delft University of Technology, Netherlands, which consisted of thin, high-strength aluminium alloy² sheets alternately bonded to plies of fibre-reinforced epoxy adhesive.

The GLARE (GLAssREinforced) FML had been developed in the same place with an improvement properties of ARALL³ in 1990. It has a better adhesion between the

glass fibres and the adhesives and provides a wide range of potential application. CARALL⁴ comprises carbon/epoxy pre-impregnated fibres adhesively bonded to the alternating layers of Al alloy. It has excellent compressive strength as compared to ARALL and is efficient in allowing crack bridging and very low fracture development. Applications of CARALL include aircraft accessories. In another version of FML (ARALL & GLARE), spliced laminates were launched by Structural Laminates Company (SLC) in 1992⁵.

In these types of FML, aluminium layers are interrupted such that the dimensions of the spliced sheets depend on the auto-clave dimensions. The new natural fibre FML has a low density and is highly economical compared to CARALL. The Jute fibre⁶ is added between the carbon fibre and Aluminium material. It is an alternative FML meant for improved corrosion resistance. Since the FMLs developed were mainly used in aerospace industries only, the application of the FMLs for marine/ocean environments is limited due to important properties like durability, corrosion and water absorption. Materials used to develop pressure housing must survive in salty environments⁷ for extended periods, a significant durability concern. While a considerable amount of information is available on the durability of Polymer Matrix Composites (PMC) for marine environments, due to the lack of a comprehensive feasibility study on the usage of FMLs in marine structures, there is no well-documented data on the durability of these materials under marine environments. The water absorption due to hygrothermal conditions can change the physical, chemical and mechanical properties of PMC, and it will not affect the FMLs much due to the outer layers being metal.

Stainless Steel (SS)-based FMLs can become the tempting choice⁸ for marine applications due to their excellent corrosion resistance. The FMLs with SS 304 and Glass/fibre epoxy exhibited better corrosion resistance and higher peel strength than mild steel-based FMLs. The FMLs comprising of a solid Glass Fiber Reinforced Plastics (GFRP) core protected by thin SS316 L layers offer excellent protection against water absorption⁹, thus preventing the loss of mechanical properties. The FMLs composed of glass fibre and protected with steel-AISI316L layers provide wear resistance and protection from moisture absorption, thereby not affecting the impact resistance of the laminate. The hardness of the steel allows for higher contact pressure, drastically increasing the wear resistance. Nonetheless, the reduced thickness of steel layers does not introduce any stress concentration at the steel-GFRP interface¹⁰.

Fibre metal laminates (FMLs), which consist of magnesium alloy layers and a continuous carbon fibre-reinforced Zn-Al¹¹ composites layer (the mass fraction of Al is 8 %), were fabricated by the diffusion bonding method. This article mainly examines the tensile behaviour of FML under various temperatures ranging from 25 °C to 175 °C, combining experimental measurement, theoretical model and numerical technique¹². The presence of steel layers in the FML sample helps¹³ increase major mechanical characteristics concerning other FML samples. The mechanical properties of Ti/CF/PMR polyamide fibre metal laminates¹⁴ with various layup

configurations and fibre layer orientation (0°, 90° and ±45°) were systematically investigated. Tensile properties of the lightweight titanium-based carbon fibre/epoxy laminates¹⁵ were investigated under Quasi-static loading. The use of polymer composite or Fiber metal laminate is still new in the development of pressure housing for subsea applications, and the same has been studied with initial finite element analysis.

2. DESCRIPTION OF THE SYSTEM

The system consists of two distinct components; (i) the sensor (hydrophone) used for passive acoustic measurements and (ii) the Data Acquisition System (DAS) with an underwater pressure vessel. Data acquisition system consists of a standalone card, real-time controller and portable storage device. The DAS enclosed in subsea pressure vessel and the power pack for continuous measurement of a minimum six months duration is shown in the Fig. 1.

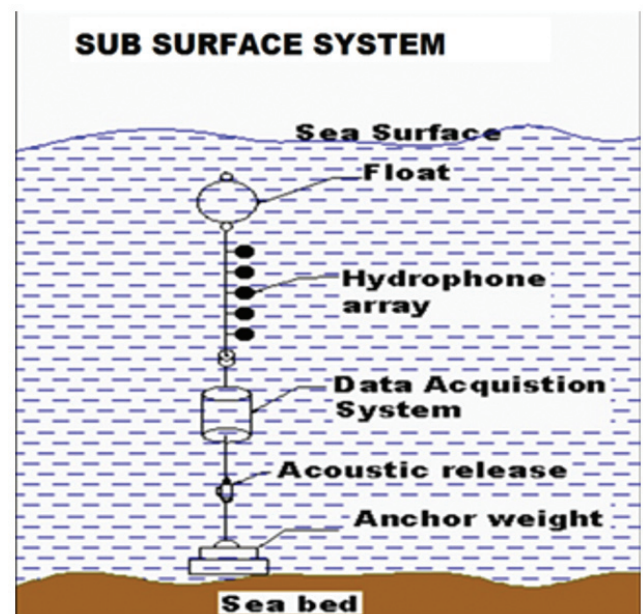


Figure 1. Subsea ambient noise measurement system.

3. METHODOLOGY

The present study involves initially the design and analysis of a pressure vessel with SS316 L alloy and subsequently the design with optimisation of a pressure vessel made of hybrid composites-FMLs, which consist of SS316 L grade metal alloy as outer layers and E-glass and Carbon fibre as inner layers. The optimisation of pressure vessels to improve structural efficiency by reducing the wall thickness of the metallic pressure housing and increasing the composite percentage in the design of subsea pressure vessels. The pressure vessel or cylinder with an external hydrostatic pressure is transformed into a rectangular plate for the FML cylinder using CLT. As preliminary measures, FML specimen with a size of 0.45 m square laminate and 0° orientation has been developed with 50 % metal layer and 50 % fibre composites, and corresponding mechanical tests have been carried out as per American Society of Testing and Materials (ASTM) standards. The results are discussed in the following sections.

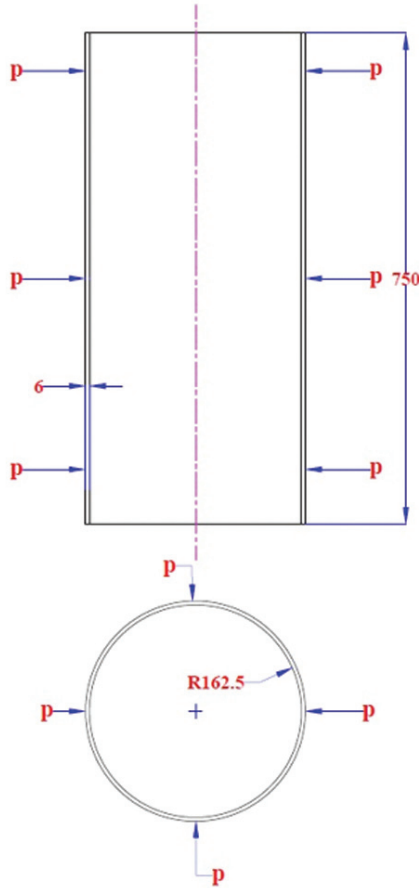


Figure 2. Hollow cylinder with pressure distribution.

4. DESIGN OF METTALLIC PRESSURE VESSEL

The thin cylinder concept is used here to design a pressure vessel. The stresses are uniform through the wall thickness. The material selected is stainless steel 316 L, and it is perfectly elastic. The Von-Mises criterion is applied to determine the minimum wall thickness of the pressure vessel. End closures are not considered in the design. Since the housing is axis-symmetric about the cylinder axis, applied pressure loading is also axis-symmetric. Consider a hollow cylinder (Fig. 2) with equilibrium in the hoop and axial direction subjected to an external hydrostatic pressure with the following geometrical properties in Table 1. The calculation of various stresses and wall thickness calculation for the pressure vessel is as follows:

- Von-Mises criterion (σ_v)

$$\sigma_v = \frac{\sqrt{3}}{2} \times \frac{p \times r}{t} \text{ in MPa} \quad (1)$$

- Wall thickness required (t)

$$t = \frac{\sqrt{3}}{2} \times \frac{p \times r}{\sigma_v} \times SF \text{ in mm} \quad (2)$$

- Failure Index (FI) for metallic materials

$$FI = \frac{\sigma_h}{\sigma_y} \leq 1 \quad (3)$$

- Longitudinal or Axial stress (σ_a)

$$\sigma_a = \frac{p \times r}{2 \times t} \text{ in MPa} \quad (4)$$

- Circumferential or Hoop stress (σ_h)

$$\sigma_h = \frac{p \times r}{t} \text{ in MPa} \quad (5)$$

- Mass(m) calculation of hollow cylinder

$$m = \rho \times \pi \times \frac{(D^2 - d^2)}{4} \times l \text{ in kg} \quad (6)$$

where, ρ = density in kg/m^3 , D =outer diameter of cylinder in mm, d =inner diameter of cylinder in mm, l = length of cylinder in mm.

Table 1. Geometric properties of metallic pressure vessel

Geometrical parameter	Specification
External pressure	1MPa
Inner radius	0.1625 m
Length	0.75 m
Factor of safety	2.0

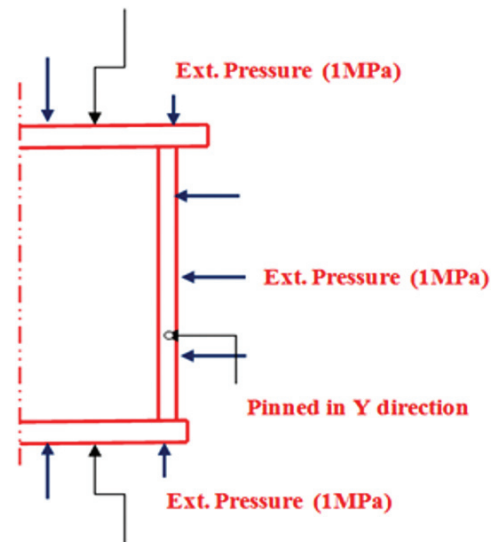
Pressure vessels operating at 100 m of ocean depth must be designed to endure the external hydrostatic pressure, drag force due to underwater current and other forces acting on the mooring system of the pressure housing. As per the Von-Mises criterion, the minimum thickness of pressure housing is 0.82 mm, whereas the Failure index (FI) exceeds unity. So, optimising the wall thickness and maintaining minimum equivalent stress is necessary. Considering all the above factors, the pressure vessel's wall thickness (t) is assumed to be 6 mm. The corresponding axial hoop stress and failure index are calculated and listed in Table 2.

Table 2. Calculation of stresses and failure Indices

σ_y -MPa	t-mm	FI	σ_a -MPa	σ_h -MPa	Mass(m)-kg
170	0.82*	1.16	99.08	198.17	4.87
170	1.64	0.58	49.54	99.08	9.78
170	3.28	0.29	24.77	49.54	19.66
170	6.0	0.159	13.54	27.08	36.26

*Without safety factor of 2 and $p=1$ MPa, where, σ_y = yield stress of the material.

x, y, z translations arrested



x, y, z translations arrested

Figure 3. Boundary Condition with free body diagram.

5. MODELING OF PRESSURE VESSEL

The cylinder is modelled with finite element analysis software ANSYS and subjected to equal external hydrostatic pressure of 1 MPa it is on all four sides at a depth of 100 m. The X, Y, and Z translations are arrested at both end caps. Since cylindrical pressure vessel is an axisymmetric model, it is pinned in Y direction at a point of the section to be revolved. The boundary condition for the actual underwater sea condition of the deployed cylindrical pressure vessel is shown in Fig. 3.

6. ANALYSIS OF METALLIC PRESSURE VESSEL

Analysis of a cylindrical pressure vessel with selected materials of Stainless steel 316 L is modelled and the corresponding results are shown in the following figure. An axisymmetric cylindrical model has been created for the Stainless steel 316 L pressure housing with solid-8node 183 elements in the ANSYS software. The symmetry boundary condition has been applied to the model for external hydrostatic pressure of 1 MPa. The Hoop stress developed (34.70 MPa) for the corresponding external hydrostatic pressure is shown in the Fig. 4.

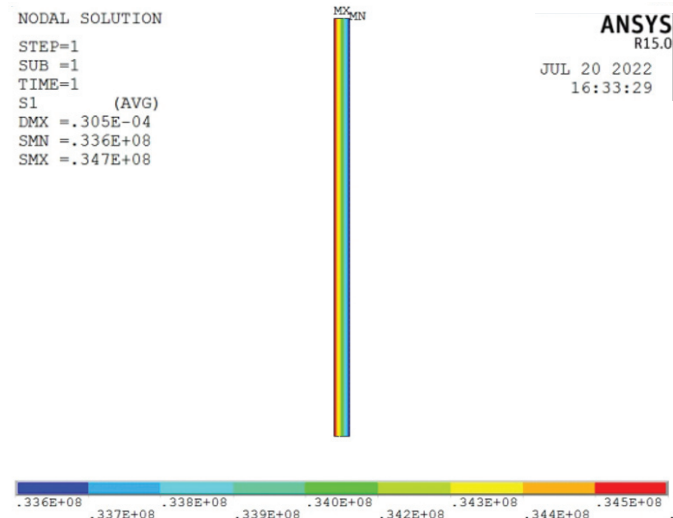


Figure 4. Hoop stress for SS316L cylinder.

7. OPTIMISED DESIGN OF PRESSURE VESSEL USING WITH HYBRID COMPOSITES

Stainless steel-based hybrid composites-FML's can become the attractive choice for ocean applications due to excellent corrosion resistance, wear resistance and protection against moisture absorption. The pressure housing considered here is made up of FML with SS316 L as outer layers and E-glass/epoxy and Carbon epoxy composite as inner layers and assumed as a cylinder. It is customary to select E-Glass fiber as reinforcement materials for marine applications. It is less weight, cost effective, strong and durable. The carbon has very advantageous of almost six times stronger than glass fiber design. Hence, combining of these materials ultimately yield the better hybrid composites or FML. Thickness of the pressure vessel has also been verified with lamina failure theories. The optimisation is process of determining the state that gives the maximum or minimum value of a function. The process includes the objective, variables and constraints.

The flow chart for the optimisation process is shown in Fig. 5. The objective of process includes design pressure, optimum wall thickness and minimum equivalent stress and variables are ply angles, ply material and varying thickness of the pressure housing range of 20 % - 80 % with an increment of 20 %. The constraints for the optimisation are Failure Index (FI) <1.0 for both metal and composites based on the Von-Mises criterion for metal and Tsai-Wu criterion for composite materials. The cylinder pressure housing or cylinder is subjected to an external hydro static pressure of 1 MPa is

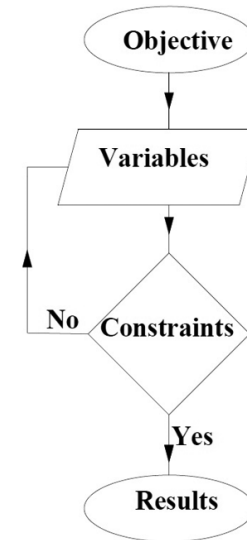


Figure 5. Flow chart for optimisation process.

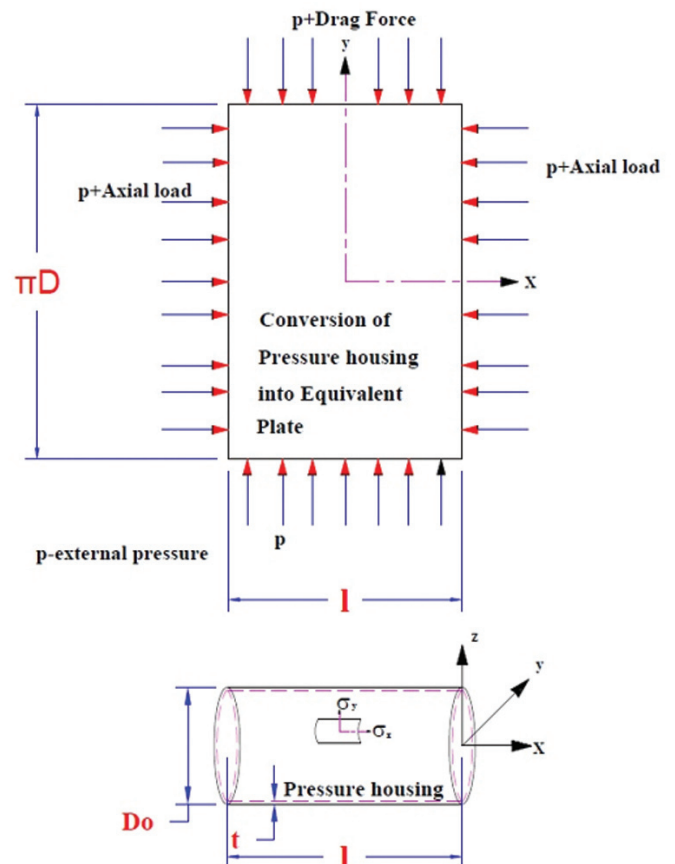


Figure 6. Conversion of cylinder into equivalent plate.

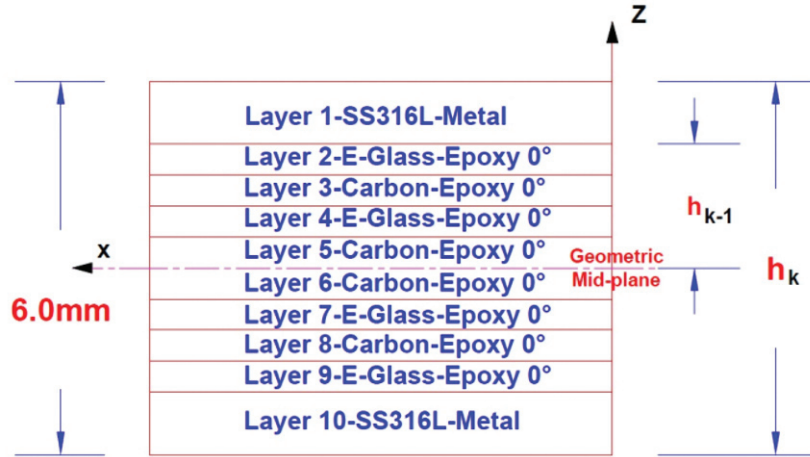


Figure 7. Orientation of FML.

Table 3. Material properties of FML

Material	ρ (kg/m ³)	γ_{12}	E_{11} (GPa)	E_{22} (GPa)	G_{12} & G_{13} (GPa)	S_{Lt} (MPa)	S_{Lc} (MPa)
SS316L	7.75	0.31	193	193	73.6	560	560
Glass fiber	1.97	0.28	41	10.4	4.3	1140	620
Carbonfiber	1.60	0.27	147	10.3	7.0	2280	57.0

γ_{12} = Poisson's ratio, E_{11} = longitudinal modulus, E_{22} = Transverse modulus, G_{12} = Shear modulus, S_{Lt} = Longitudinal strength and S_{Lc} = Compressive strength

Table 4. Combinations of FML

Combinations	Per cent of metal layer thickness (mm)	Per cent of composite (E-glass+carbon fibers) layers thickness (mm)
C1	80-4.8	20-1.2
C2	60-3.6	40-2.4
C3	40-2.4	60-3.6
C4	28-1.68	72-4.32

transformed on to a rectangular plate with stress & moment resultants in both x and y directions as shown in the below Fig. 6. Once it is converted to rectangular coordinate system by using classical lamination theory against the external hydro static pressure developed outside the cylinder is assumed as 1 MPa to calculate the stresses in different layer of the pressure vessel.

8. LAYER ORIENTATION OF COMPOSITE LAMINATE

The FML pressure vessel's total thickness is 6mm for SS316 L metallic pressure housing. The weight reduction of metal is varied from 28 % to 80 % with the wall thickness of the cylinder. The minimum metal layer thickness is 1.68 mm, and the maximum is 4.8mm. E-glass and carbon layers of equal quantities are used at the inner layers with unidirectional orientation. The orientation of FML is shown in Fig.7.

9. ABD MATRIX CALCULATIONS

Force and Moment resultant, ABD Matrix and Stresses in each layer of composites have been calculated using the FML material properties as specified in Table 3. In the FML, laminate stresses in each layer are theoretically calculated using Classical Laminated Theory (CLT).

9.1 Force and Moment Resultant

Force and Moment resultants acting on the equivalent plate per unit width in X& Y direction are calculated as follows:

$$N_X = \frac{p \times d}{4} = \frac{1 \times 325}{4} = 81.25 \text{ in N/mm} \quad (7)$$

$$N_Y = \frac{p \times d}{2} = \frac{1 \times 325}{2} = 162.5 \text{ N/mm} \quad (8)$$

$$M_X = N_X \times z = 81.25 \times 6 = 487.5 \text{ N-mm} \quad (9)$$

$$M_Y = N_Y \times z = 162.5 \times 6 = 975 \text{ N-mm} \quad (10)$$

where, N_x =Normal force resultant in x-direction, N_y =Normal force resultant in y-direction, M_x = Bending moment resultant in x-direction, M_y = Bending moment resultant in y-direction=inner diameter of cylinder in mm, Z =wall thickness of cylinder in mm.

9.2 Force and Moment Resultants are Given

$$\begin{Bmatrix} N \\ M \end{Bmatrix} = \begin{bmatrix} A & B \\ B & D \end{bmatrix} \begin{Bmatrix} \epsilon^o \\ \kappa^o \end{Bmatrix} \quad (11)$$

where, A =Extensional stiffness matrix, B=Coupling Matrix and D=Bending Stiffness Matrix, ϵ^o =midplane strain and κ^o = mid plane curvature

9.3 Q-Matrix for Glass/Carbon epoxy

$$Q_{11} = \frac{E_{11}}{[1 - \gamma_{12} \times \gamma_{21}]} \quad (12)$$

$$Q_{22} = \frac{E_{22}}{[1 - \gamma_{12} \times \gamma_{21}]} \quad (13)$$

$$Q_{12} = \frac{E_{22} \times \gamma_{12}}{[1 - \gamma_{12} \times \gamma_{21}]} \quad (14)$$

$$Q_{13} = Q_{31} = Q_{23} = Q_{32} = 0 \quad (15)$$

$$Q = \begin{bmatrix} Q_{11} & Q_{12} & Q_{13} \\ Q_{21} & Q_{22} & Q_{23} \\ Q_{31} & Q_{32} & Q_{33} \end{bmatrix} \text{GPa} \quad (16)$$

where, Q=Stiffness Matrix, γ =Poisson's ratio

9.4 Q-Matrix for Stainless Steel-316L-GPa

$$Q = \begin{bmatrix} \frac{E}{1-\gamma^2} & \frac{\gamma \times E}{1-\gamma^2} & 0 \\ \frac{\gamma \times E}{1-\gamma^2} & \frac{E}{1-\gamma^2} & 0 \\ 0 & 0 & G \end{bmatrix} \quad (17)$$

Finding [A], [B] and [D] matrices,

9.5 Calculation of 'A' Matrix

$$A_{ij} = \sum_{k=1}^n (Q_{ij})_k (z_k - z_{k-1}) \quad (18)$$

9.6 Calculation of 'B' Matrix

$$B_{ij} = \frac{1}{2} \sum_{k=1}^n (Q_{ij})_k (Z_k^2 - Z_{k-1}^2) \quad (19)$$

B=0 (Since Symmetric laminates)

9.7 Calculation of 'D' Matrix

$$D_{ij} = \frac{1}{3} \sum_{k=1}^n (Q_{ij})_k (Z_k^3 - Z_{k-1}^3) \quad (20)$$

9.8 Calculation of 'ABD' Matrices

$$\begin{pmatrix} N_X \\ N_Y \\ N_{XY} \\ M_X \\ M_Y \\ M_{XY} \end{pmatrix} = \begin{bmatrix} A_{11} & A_{12} & A_{13} & 0 & 0 & 0 \\ A_{21} & A_{22} & A_{23} & 0 & 0 & 0 \\ A_{31} & A_{32} & A_{33} & 0 & 0 & 0 \\ 0 & 0 & 0 & D_{11} & D_{12} & D_{13} \\ 0 & 0 & 0 & D_{21} & D_{22} & D_{23} \\ 0 & 0 & 0 & D_{31} & D_{32} & D_{33} \end{bmatrix} \begin{pmatrix} \varepsilon_x^o \\ \varepsilon_y^o \\ \gamma_{xy}^o \\ K_x^o \\ K_y^o \\ K_{xy}^o \end{pmatrix} \quad (21)$$

9.9 Stress Resultants Acting on Composites

$$\begin{pmatrix} N_X \\ N_Y \\ N_{XY} \end{pmatrix} = \begin{bmatrix} A_{11} & A_{12} & A_{13} \\ A_{21} & A_{22} & A_{23} \\ A_{31} & A_{32} & A_{33} \end{bmatrix} \begin{pmatrix} \varepsilon_x^o \\ \varepsilon_y^o \\ \varepsilon_{xy}^o \end{pmatrix} + \begin{bmatrix} B_{11} & B_{12} & B_{13} \\ B_{21} & B_{22} & B_{23} \\ B_{31} & B_{32} & B_{33} \end{bmatrix} \begin{pmatrix} K_x^o \\ K_y^o \\ K_{xy}^o \end{pmatrix} \quad (22)$$

Since the coupling matrix [B]=0, the in plane strains can be calculated with the calculated N_x and N_y values as follows:

$$\begin{pmatrix} \varepsilon_x^o \\ \varepsilon_y^o \\ \gamma_{xy}^o \end{pmatrix} = [A]^{-1} \times \{N\} \quad (23)$$

9.10 Moment Resultants Acting on Composite

$$\begin{pmatrix} M_X \\ M_Y \\ M_{XY} \end{pmatrix} = \begin{bmatrix} B_{11} & B_{12} & B_{13} \\ B_{21} & B_{22} & B_{23} \\ B_{31} & B_{32} & B_{33} \end{bmatrix} \begin{pmatrix} \varepsilon_x^o \\ \varepsilon_y^o \\ \varepsilon_{xy}^o \end{pmatrix} + \begin{bmatrix} D_{11} & D_{12} & D_{13} \\ D_{21} & D_{22} & D_{23} \\ D_{31} & D_{32} & D_{33} \end{bmatrix} \begin{pmatrix} K_x^o \\ K_y^o \\ K_{xy}^o \end{pmatrix} \quad (24)$$

Since the coupling matrix [B]=0, the in plane curvature can be calculated as follows:

$$\{K^0\} = [D]^{-1} \times \{M\} \quad (25)$$

9.11 Stresses in Principal Coordinate System for Each Layer

$$\begin{pmatrix} \sigma_X \\ \sigma_Y \\ \tau_{XY} \end{pmatrix} \begin{bmatrix} Q_{11} & Q_{12} & Q_{13} \\ Q_{21} & Q_{22} & Q_{23} \\ Q_{31} & Q_{32} & Q_{33} \end{bmatrix} \begin{pmatrix} \varepsilon_x^o \\ \varepsilon_y^o \\ \gamma_{xy}^o \end{pmatrix} + z \begin{pmatrix} K_x^o \\ K_y^o \\ K_{xy}^o \end{pmatrix} \quad (26)$$

9.12 Stresses in the Material Coordinate System for Each Layer

$$\begin{pmatrix} \sigma_1 \\ \sigma_2 \\ \sigma_3 \end{pmatrix} = [T_\sigma] \begin{pmatrix} \sigma_X \\ \sigma_Y \\ 0 \end{pmatrix} = \begin{bmatrix} m^2 & n^2 & 2mn \\ n^2 & m^2 & -2mn \\ -mn & mn & m^2 - n^2 \end{bmatrix} \begin{pmatrix} \sigma_X \\ \sigma_Y \\ 0 \end{pmatrix} \text{MPa} \quad (27)$$

Where $m = \cos\theta$ and $n = \sin\theta$

10. FAILURE STRENGTH PREDICTION OF FML

The Tsai-wu criterion is used to predict the failure of composites of different layers. The Von-Mises criterion is used for metal layers. The failure of FML can be expressed as¹⁶.

$$\text{Max}[f(\theta_f), f(\theta_m)] = 1 \quad (28)$$

where, θ_f =Failure Index of composite layer and θ_m = Failure Index of metal layer

10.1 Failure Index Corresponding to Tsai-wu Criterion in Composite Layer

$$F(\theta_f) = F_{11}\sigma_1^2 + F_{22}\sigma_2^2 + F_{33}\sigma_3^2 + 2F_{12}\sigma_1\sigma_2 + 2F_{23}\sigma_2\sigma_3 + 2F_{13}\sigma_1\sigma_3 + F_{44}\tau_{12}^2 + F_{55}\tau_{23}^2 + F_{66}\tau_{13}^2 + F_1\sigma_1 + F_2\sigma_2 + F_3\sigma_3 \quad (29)$$

Where, $F_{11} = \frac{1}{X_T X_C}$; $F_{22} = \frac{1}{Y_T Y_C}$; $F_{33} = \frac{1}{X_T X_C}$; $F_{44} = \frac{1}{R^2}$; $F_{55} = \frac{1}{S^2}$;

$$F_{66} = \frac{1}{T^2}; F_1 = \frac{1}{X^T} - \frac{1}{X^C}; F_2 = \frac{1}{Y^T} - \frac{1}{Y^C}; F_3 = \frac{1}{Z^T} - \frac{1}{Z^C}; F_{12} = -0.5\sqrt{F_{11}F_{22}}; F_{23} = -0.5\sqrt{F_{22}F_{33}}; F_{13} = -0.5\sqrt{F_{11}F_{33}}$$

where, X_T and X_C - tensile and compressive strength along the fiber direction, Y_T and Y_C - tensile and compressive strength along the transverse direction, R and T-out of plane shear strengths, S-in plane shear strength.

10.2 Failure Index Corresponding to Von-Mises Criterion in FML

$$F(\theta_m) = \frac{1}{\sigma_y} \left((\sigma_x^2 + \sigma_y^2 + \sigma_z^2) - (\sigma_x\sigma_y + \sigma_x\sigma_z + \sigma_y\sigma_z) + 3(\tau^2_{xy} + \tau^2_{xz} + \tau^2_{zy}) \right)^{1/2} \quad (30)$$

The failure index values are calculated using the suitable failure criteria, and Tsai-wu for composite layers and Von-Mises criterion for metal layers have been used. FML are categorised as metal and composite layer combinations with the following combinations as listed in Table 4. The determined results of the CLT using Autocad-Helius software are tabulated in Table 5.

11. ANALYSIS OF FML PRESSURE HOUSING

A finite element modelling of the composite cylinder has been carried out using 183 solid elements in ANSYS for the FML-composite part with axisymmetric analysis. The FML composite pressure housing consisting of a cylinder made up of SS316L, E-glass/epoxy and Carbon fibre layers with a stacking sequence of (0/0/0/0/0)s has been considered. It is

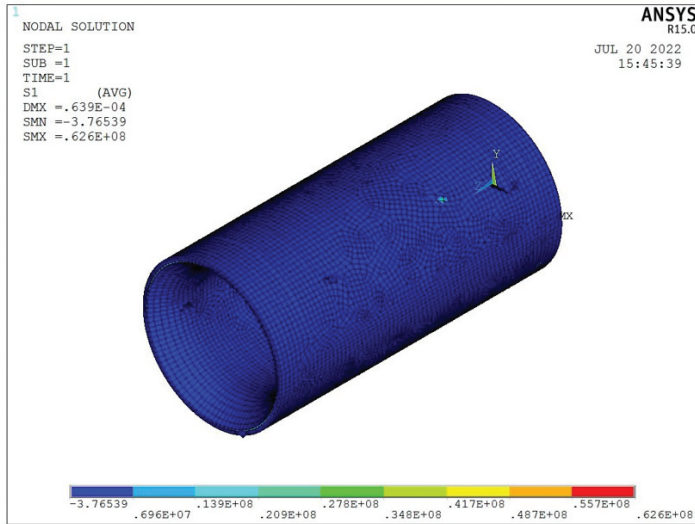


Figure 8. Hoop stress of FML pressure housing.

shown in Fig. 7. The X, Y, and Z translations are arrested at both ends and subjected to an external hydrostatic of 1 MPa. The corresponding hoop stress obtained for 40 % metal layer combinations (C3) is shown below in Fig. 8.

12. EXPERIMENTAL ANALYSIS

The FML was fabricated with 50 % of metal layer and 50 % fiber resin composites. The SS316L/Glass/carbon/SS316L FML was fabricated by hand lay-up process and later followed with compression molding machine. The volume fraction ratio of fiber and resin was 50:50. The unidirectional FML were arranged with sequence of SS316L/G/C/G/C/G/C/G/C/G/SS316 L. The surface of the SS316 L are etched with proper surface preparation for binding.

Normally rough surface will get good bonding strength. Bondite super strength adhesive were used for the bonding of metal and composite panels. The fabricated panels have dimensions 450x450x6.06 mm. The panels were cut using abrasive water jet with various sizes as per ASTM standards for various testing like Tension, Flexural and Impact. The

fabricated FML specimen for testing are shown in the Fig. 9(a) - Fig. 9(c). Five test specimens of FML and the base metal of SS316 L were prepared for various testing like tensile, flexural and impact as per ASTM standards for accurate results. The specimens (coupon) were prepared with constant cross section of rectangular shape.

Tensile test as per ASTM D3039 was carried out with specimen dimensions of 250x15x6 mm for all the five specimens in the FIE make Universal Testing Machine (UTM) with a capacity of 100 KN. Three point flexural test as per ASTM D 790 was carried out with 50KN capacity UTM for the five specimens with a size of 80x13x5 mm. Similarly, Izod impact tests as per ASTM D256 were done in the impact pendulum testing machine of capacity 100 Joules. The test results obtained for the various tests like tensile, flexural and Impact was considered for the analysis. Five specimens were used for testing and to get the average strength of the FML specimen. Figure 10(a) represents the tensile results of the FML specimen. The stress-strain curve indicates a lower strain value of 0.25 mm to a higher strain value of 1.60 mm for the corresponding stress value. The peak value of the stress is lesser (420.76 MPa) than the base metal (SS316L), with an ultimate stress of 556.05 MPa, and the average stress value of the FML is 253.07 MPa. The tensile specimen failure of SS FML occurred in three steps. First, the inner glass and carbon fibre epoxy sheet failed at an ultimate tensile load of 42KN with an ultimate stress of 420 MPa. After that, outer stainless steel sheets failed one after another with considerable strain. The tensile stress-displacement of interfacial behaviour SS316L FML is shown in Fig. 10(b). The result shows a better improvement in the ultimate tensile load with a combination of SS316L FML and glass and carbon fibre compared to the other types of FMLs. The flexural results of the specimen are shown in Figure 10c, with a maximum stress value of FML of 130MPa with a strain value of 0.05. The maximum value of the FML specimen with low velocity impact test is 82 joules when compared to all other FML specimens, and the impact results are shown in Fig. 10(d).



(a)



(b)



(c)

Figure 9. (a) Tensile test specimen; (b) Flexural test specimen; and (c) Impact test specimen.

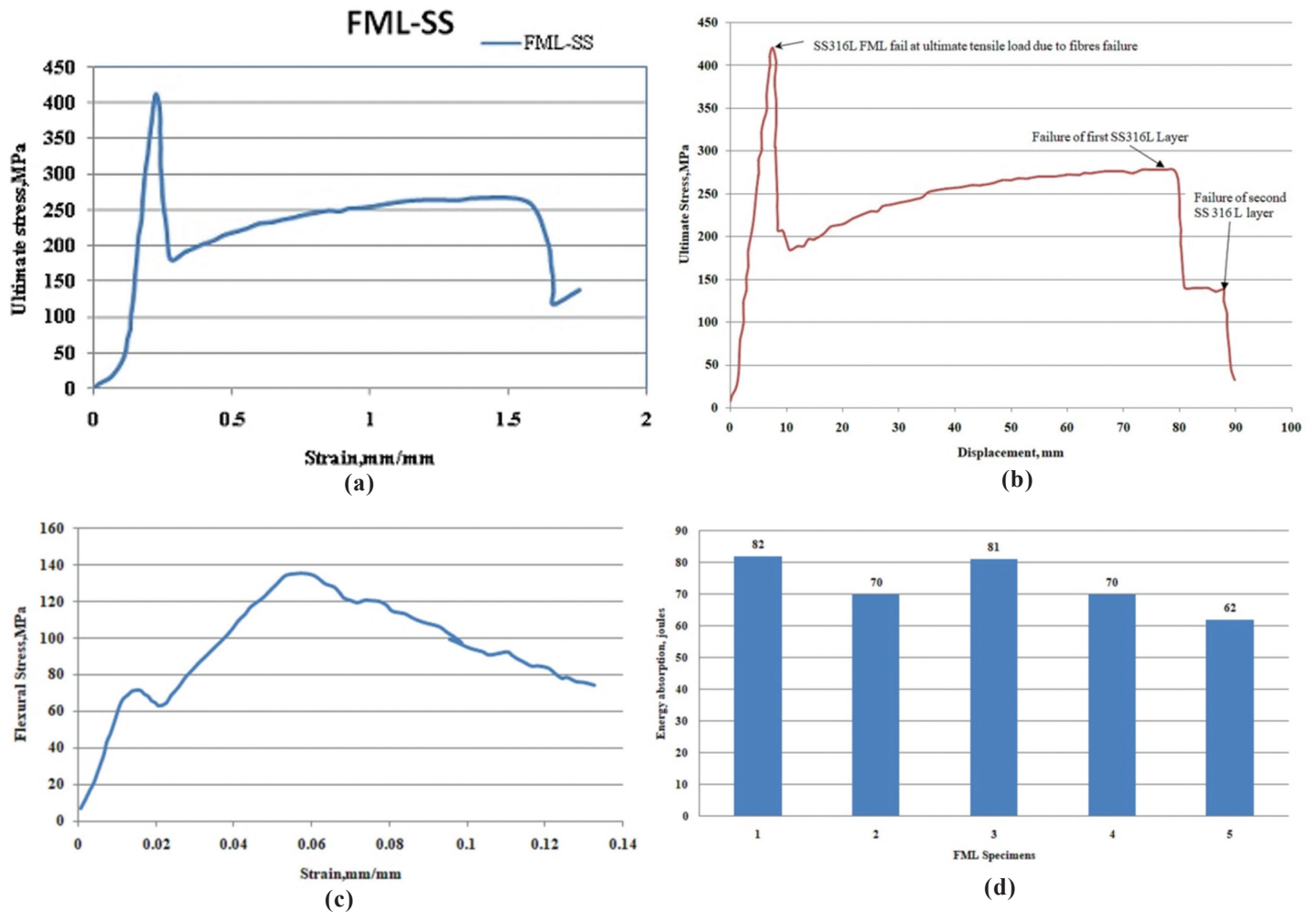


Figure 10. (a) Tensile test results: Stress-Strain graph; (b) Stress-displacement behavior of FML; (c) Flexural test results: Stress-Strain graph; and (d) Impact test results.

It has been observed that the proposed FML possess excellent flexural and Impact properties considering the other kind of Fiber metal laminates like ARALL, CARALL and GLARE. Combining E-glass and carbon fibre with SS316L is more advantageous for tensile and Impact strength.

13. RESULTS AND DISCUSSION

Classical laminated theory calculates the stresses for FML of different combinations along the fibre and transverse directions. In the FML, with stacking of metallic layer and unidirectional composites of glass and carbon fibres are subjected to force resultant of 81.25N/mm. The Tsai-wu criterion calculates failure index values in all the layers composites. In the 0° orientation of glass and carbon laminates, the failure index values range from 0.007 to 0.02. For metal layers, the Von-Mises criterion is used. Earlier research studies found that FMLs with (0/90°) orientation composites have maximum Von-Mises stress and least radial stress for the composite layer thickness¹⁸. The failure index for the Metal layers is in the range of 0.204-0.530. Similarly, the stresses and failure index is calculated with Autodesk-Helius composite software and listed in Table 5. It has been observed that results are very close with different combinations of FML. The optimum FI and stress values occur at 40 % of the metallic layer for the given

force resultant. The wall thickness of the pressure housing is 1.2 mm, which satisfies the Von-Mises criterion. FMLs with a 50 % metal layer are currently experimentally developed based on commercially available materials. The unfavourable FI and stress values occur in less than 28 % of metal layer combinations. In order to validate, the stress predicted by FEA-ANSYS for FML is compared with theoretically calculated values of both CLT and Helius composite software. It is found that the results of optimization agree very closely, which is shown in Table 5.

14. CONCLUSIONS

- The design optimisation of FML Pressure housing with different combinations of metal layers and composites using CLT theory is calculated and compared with finite element modelling and analysis tools.
- Theoretically, the objective of reducing the mass of pressure housing with FML has been achieved with a combination (C3) of 40 % metal layer and 60 % composite layers with 0° fibre orientation of composites.
- The total mass of the pressure housing with FML was reduced to 20.0 kg against the pressure housing with metal of 36 kg.
- The experimental results of the FML specimens with a 50 % metal layer combination show that the developed

Table 5. Comparison of values with CLT, helius & ansys

Comb.	Σ_x and Σ_y (Mpa) and Fi	CLT	Helius-composites	FEA-ANSYS	Housing mass (kg)
C1	Metal layers	$\Sigma_x=16.7$	$\Sigma_x=16.7$	$\Sigma_x=18.2$	30.6
		$\Sigma_y=34.7$	$\Sigma_y=34.6$	$\Sigma_y=35.2$	
		$\Gamma_{xy}=0$	$\Gamma_{xy}=0$	$\Gamma_{xy}=0$	
	F.I	0.203	0.204	0.226	
	Glass Layers	$\Sigma_x=1.60$	$\Sigma_x=1.74$	$\Sigma_x=1.92$	
		$\Sigma_y=1.40$	$\Sigma_y=1.75$	$\Sigma_y=1.86$	
		$\Gamma_{xy}=0$	$\Gamma_{xy}=0$	$\Gamma_{xy}=0$	
	F.I	0.023	0.014	0.020	
	Carbon Layers	$\Sigma_x=5.01$	$\Sigma_x=5.07$	$\Sigma_x=5.27$	
		$\Sigma_y=1.73$	$\Sigma_y=1.70$	$\Sigma_y=1.80$	
		$\Gamma_{xy}=0$	$\Gamma_{xy}=0$	$\Gamma_{xy}=0$	
	F.I	0.006	0.007	0.0068	
C2	Metal Layers	$\Sigma_x=20.8$	$\Sigma_x=20.7$	$\Sigma_x=21.0$	24.8
		$\Sigma_y=45.4$	$\Sigma_y=45.2$	$\Sigma_y=46.3$	
		$\Gamma_{xy}=0$	$\Gamma_{xy}=0$	$\Gamma_{xy}=0$	
	F.I	0.266	0.267	0.272	
	Glass Layers	$\Sigma_x=1.80$	$\Sigma_x=2.2$	$\Sigma_x=2.2$	
		$\Sigma_y=1.80$	$\Sigma_y=2.1$	$\Sigma_y=2.2$	
		$\Gamma_{xy}=0$	$\Gamma_{xy}=0$	$\Gamma_{xy}=0$	
	F.I	0.0189	0.0190	0.0185	
	Carbon Layers	$\Sigma_x=5.76$	$\Sigma_x=5.83$	$\Sigma_x=5.76$	
		$\Sigma_y=2.76$	$\Sigma_y=2.24$	$\Sigma_y=2.34$	
		$\Gamma_{xy}=0$	$\Gamma_{xy}=0$	$\Gamma_{xy}=0$	
	F.I	0.0094	0.009	0.0089	
C3	Metal Layers	$\Sigma_x=28.2$	$\Sigma_x=28.0$	$\Sigma_x=29.0$	20
		$\Sigma_y=65.7$	$\Sigma_y=65.1$	$\Sigma_y=62.6$	
		$\Gamma_{xy}=0$	$\Gamma_{xy}=0$	$\Gamma_{xy}=0$	
	F.I	0.203	0.204	0.226	
	Glass Layers	$\Sigma_x=2.34$	$\Sigma_x=2.55$	$\Sigma_x=2.75$	
		$\Sigma_y=2.66$	$\Sigma_y=3.23$	$\Sigma_y=3.46$	
		$\Gamma_{xy}=0$	$\Gamma_{xy}=0$	$\Gamma_{xy}=0$	
	F.I	0.0176	0.020	0.0184	
	Carbon Layers	$\Sigma_x=6.85$	$\Sigma_x=6.90$	$\Sigma_x=6.98$	
		$\Sigma_y=3.29$	$\Sigma_y=3.21$	$\Sigma_y=3.58$	
		$\Gamma_{xy}=0$	$\Gamma_{xy}=0$	$\Gamma_{xy}=0$	
	F.I	0.0135	0.0130	0.0134	
C4	Metal Layers	$\Sigma_x=36.5$	$\Sigma_x=36.1$	$\Sigma_x=37.2$	15.64
		$\Sigma_y=89.8$	$\Sigma_y=88.9$	$\Sigma_y=89.0$	
		$\Gamma_{xy}=0$	$\Gamma_{xy}=0$	$\Gamma_{xy}=0$	
	F.I	0.522	0.528	0.530	
	Glass Layers	$\Sigma_x=2.7$	$\Sigma_x=3.04$	$\Sigma_x=3.14$	
		$\Sigma_y=3.6$	$\Sigma_y=4.40$	$\Sigma_y=4.20$	
		$\Gamma_{xy}=0$	$\Gamma_{xy}=0$	$\Gamma_{xy}=0$	
	F.I	0.0289	0.0292	0.0295	
	Carbon Layers	$\Sigma_x=7.8$	$\Sigma_x=7.87$	$\Sigma_x=7.92$	
		$\Sigma_y=4.5$	$\Sigma_y=4.38$	$\Sigma_y=4.55$	
		$\Gamma_{xy}=0$	$\Gamma_{xy}=0$	$\Gamma_{xy}=0$	
	F.I	0.0175	0.0171	0.078	

FML has a comparable tensile strength (420 Mpa) with the base metal SS316 L tensile strength (556 MPa). Flexural and Impact properties have shown a higher level when compared to other FMLs like ARALL, CARALL and GLARE¹⁷.

- The experiment on FML specimens with hygrothermal conditioning with 40° and 70 °C temperatures with normal and sea water is planned to check and compare water percolation (water absorption).
- The testing of FML subjected to external hydrostatic pressure for 1MPa and High/low temperature is conducted, and the test results show prominent results compared to other types of FMLs.
- SS316L-based FMLs are the tempting choice for marine applications due to their excellent corrosion resistance, strength-to-weight ratio, wear resistance and protection against moisture absorption.
- The developed FML is ultimately suitable for the developing pressure vessels for Ocean applications and offshore structures.

REFERENCES

1. Thirunavukkarasu, A.; Latha, G. & Shanmugasundaram. K. Design of subsea pressure housing for ambient noise measurement system in the Arctic region. *OCEANS 2022 - Chennai*, Chennai, India, 2022, 1-6. doi: 10.1109/OCEANSSChennai45887.2022.9775471.
2. Asundi, A. & Alta, Y.N. Choi. Fiber metal laminates: An advanced materials for future aircraft. *J. Mater. Proc. Tech.*, 1997, **63**, 384-394. doi: 10.1016/S0924-0136(96)02652-0.
3. Krishna Kumar, S. Fiber metal laminates-The synthesis of metals and composites. *J. Mater. Manu. Proc.*, 1994, **9(2)**, 295-354. doi: 10.1080/10426919408934905.
4. Chandrasekar, M.; Ishak, M.R.; Jawaid, M.; Leman, Z. & Sapuan, S.M. An experimental review on the mechanical properties and hygrothermalbehaviour of fibre metal laminates. *J. Rein. Plast. Comp.*, 2016, **1**, 1-11. doi:10.1177/07316844166668.
5. Tamer, S.; Egemen, S.A.; Mustafa, O. & Onur, C. A review: Fibre metal laminates, background, bonding types and applied test methods. *Mater. Des.*, 2011, **32**, 3671-3685. doi:10.1016/j.matdes.2011.03.011.
6. Vasumathi, M. & Velamurali. Effect of alternate metals for use in natural fibre reinforced fibre metal laminates under bending, impact and axial loadings. *Pro. Eng.*, 2013, **64**, 562-570. doi: 10.1016/j.proeng.2013.09.131.
7. Najafi, M.; Darvizeh, A. & Ansari, R. Effect of salt water conditioning on novel fiber metal laminates for marine applications. *J. Mater. Des. appln.*, 2018, **1**, 1-13. doi: 10.1177/14644207187679.
8. Meng, M.; Rizvi, M.D.J.; Grove, S. & Le, H.R. Effects of hygrothermal stress on the failure of CFRP composites. *J. Comp. Struct.*, 2015, **133**, 1024-1035. doi: 10.1016/j.compstruct.2015.08.016.
9. Satnam, S. & Surjit, S. Experimental evaluation of hygrothermal degradation of stainless steel fibre metal laminate. *Eng. Sci. Tech.*, 2018, **21**, 170-179. doi: 10.1016/j.jestch.2018.01.002.
10. Poodts, E.; Ghelli, D.; Brugo, T.; Panciroli, R. & Minak, G. Experimental characterization of a fiber metal laminate for underwater applications. *Comp. Struct.*, 2015, **129**, 36-46. doi: 10.1016/j.compstruct.2015.03.046.
11. Xinwei, H.; Huihui, N.; Zhe, Y.; Yi, L.; Liu, W.Z. & Wei, L. Mechanical properties of a novel fiber metal laminates based on a carbon fiber reinforced Zn-Al alloy composite. *Mater. Sci. Eng. A.*, 2019, **740-741**, 218-225. doi: 10.1016/j.msea.2018.10.050.
12. Lu, Y.; Shaofeng, Z.; Xiaojian, C.; Zhenyuan, G.; Changzi, W. & Wentou, H. Tensile behaviour and failure mechanism of fiber metal laminates under various temperature environments. *Comp. Struct.*, 2022, **284**, 115-142. doi:10.1016/j.compstruct.2021.115142.
13. Khalili, S.M.R.; Mittal, R.K. & Gharibi, C.S. A study of the mechanical properties of Steel/Aluminium/GRP Laminates. *Mater. Sci. Eng A.*, 2005, **412**, 137-140. doi: 10.1016/j.msea.2005.08.016.
14. Yubing, H.; Yanan, Z.; Xuelong, F. & Wei, J. Mechanical properties of Ti/CF/PMR polyimide fiber metal laminates with various layup configurations. *Comp. Struct.*, 2019, **229**, 111408. doi: 10.1016/j.compstruct.2019.111408.
15. Jing, S.; Ali, D.; Guoxing, L.; Dong, R. & Yang, L. Tensile failure of fibre metal laminates made of titanium and carbon fibre/epoxy laminates. *Mater. Des.*, 2019, **183**, 108-139. doi: 10.1016/j.matdes.2019.108139.
16. Rajesh, K.M.; Danish, A.R.; Tamilan, K. & Gibreel, A.H.M. Computation of failure Index strength of FML and FRP composites. *Int. Res. J. Eng. Tech.*, 2018, **5(10)**, 2313-2320. <https://irjet.net/archives/V5/i3/IRJET-V5I3530>. (Accessed on 17 September 2020).
17. Boopathy, G.; Vijayakumar, K.R.; Chinnapandian, M. & Gurusamy, K. Development and experimental characterisation of fiber metal laminates to predict fatigue life. *Int. J. Inno. Tech. Exp. Eng.*, 2019, **8(10)**, 2815-2818. doi: 10.35940/ijtee.J9597.0881019
18. Sumana, B.G.; Vidyasagar, H.N.; Sharma, K.V. & Krishna, M. Numerical analysis of stresses on layer-layer basis in FML composite cylinder subjected to external hydrostatic loading. *Mater. Sci. Appln.*, 2015, **6**, 489-499. doi: 10.4236/msa.2015.66052

ACKNOWLEDGEMENT

We sincerely thank the Director, NIOT for his constant support and encouragement. We are thank to Ministry of Earth Sciences for funding this research work. We immensely thank our team members in the Ocean Acoustics group of NIOT for supporting us at various stages in the successful completion of the project.

CONTRIBUTORS

Mr A. Thirunavukkarasu is working as a Scientific Officer with a specialisation of mechanical engineering at Ocean Acoustics, National Institute of Ocean Technology, Chennai. He is currently doing the PhD program under Engineering Design division at College of Engineering, Guindy, Anna University, Chennai. He is involved in the design and development of underwater pressure vessel and its components with marine grade materials for the development of autonomous ambient noise measurement system in shallow waters of Indian seas including for the Polar region. In the current study he has designed and developed the hybrid composites and prepared the manuscript.

Dr K. Shanmugasundaram obtained his PhD in Engineering from Design Division, College of Engineering, Anna University and he is working as a Professor at College of Engineering, Guindy, Anna University, Chennai. His areas of interest include: Design of hydraulic and pneumatic systems, machine design, finite element analysis, computer aided design, product design and development, additive manufacturing and metal matrix composites.

In the current study, he has worked on the presentation of experiment results and reviewed the manuscript.

Dr G. Latha obtained her PhD in Mathematics from IIT, Madras and she is working as Scientist-G and Head, Ocean Acoustics, National Institute Ocean Technology, Chennai. Her research areas of expertise include: Ocean acoustics and modelling of ocean processes.

In the current study, she worked on the presentation of simulation results and overall review of the manuscript.